STUDY OF THE DALITZ PLOT OF THE $\eta \to \pi^+\pi^-\pi^0$ DECAY WITH THE KLOE DETECTOR*

Li Caldeira Balkeståhl

on behalf of the KLOE-2 Collaboration

Uppsala University, Department of Physics and Astronomy
Box 516, 751 20 Uppsala, Sweden

The decay $\eta \to \pi^+\pi^-\pi^0$ is studied with the KLOE detector, at the DAΦNE e^+e^- collider. Using a data sample corresponding to an integrated luminosity of 1.6 fb^{-1}, a new study of the Dalitz plot is presented.

1. Introduction

The isospin violating decay $\eta \to 3\pi$ is a good laboratory to study the light-quark mass difference, $m_d - m_u$. According to Sutherland and Bell [1, 2], the electromagnetic contributions to this decay are small. Calculations of the electromagnetic corrections in chiral perturbation theory (χPT) at next-to-leading order (NLO), at the isospin limit, $\mathcal{O}(e^2)$ [3] and including isospin breaking to leading order, $\mathcal{O}(e^2(m_d - m_u))$ [4], show only small effects, confirming Sutherland and Bell's conclusions. The $\eta \to 3\pi$ decay thus proceeds mainly by strong interactions and the process can be calculated in χPT. Up to NLO, the decay rate of $\eta \to \pi^+\pi^-\pi^0$ is related to the quark mass ratio Q as follows:

$$\Gamma\left(\eta \to \pi^+\pi^-\pi^0\right) \propto Q^{-4}\,, \qquad Q^2 \equiv \frac{m_s^2 - \hat{m}^2}{m_d^2 - m_u^2}\,, \qquad \hat{m} = \tfrac{1}{2}(m_d + m_u)\,.$$

As can be seen from the definition of Q, if one neglects the small term $\hat{m}^2/m_s^2$, the formula becomes an ellipse in the $\frac{m_s}{m_d}, \frac{m_u}{m_d}$ plane with major semi-axis Q, the Leutwyler ellipse [5], shown in Fig. 1. A precise knowledge of Q is an important constraint for the light quark masses.
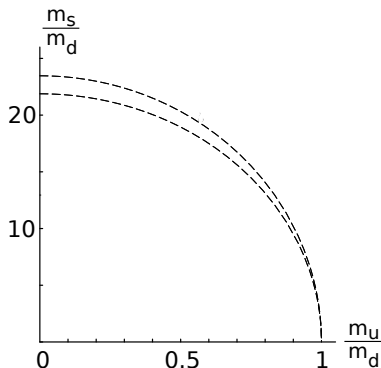

Fig. 1. The Leutwyler ellipse shows the constraints for the light quark masses, here for $Q = 22.7 \pm 0.8$.

At leading order in χPT, Q can be extracted from meson masses. Assuming Dashen's theorem [6] to fix the electromagnetic contribution to the meson masses gives $Q \equiv Q_{\mathrm{D}} = 24.2$. Using Q_{D} in LO and NLO χPT calculations results in values of the decay width $\Gamma(\eta \to \pi^+\pi^-\pi^0)$ not in agreement with the experimental value: $\Gamma_{\mathrm{LO}} = 66$ eV, $\Gamma_{\mathrm{NLO}} = 160 \pm 50$ eV [7] (updated to $\Gamma_{\mathrm{NLO}} = 168 \pm 50$ eV [5]) and $\Gamma_{\mathrm{exp}} = 295 \pm 16$ eV [8].

The big difference between LO and NLO results indicates a slow convergence of the χPT series and the importance of final state interaction between pions. Instead of using Q to predict the decay width, an accurate theoretical calculation of the decay amplitude together with an accurate experimental value for the decay width can be used to extract Q.

There have been several efforts on improving the decay amplitude calculations. An NNLO χPT calculation was performed by Bijnens and Ghorbani (in leading order isospin breaking) [9], but at this order many Low Energy Constants must be fixed. Dispersion relations can be used to take into account the $\pi\pi$ interactions, and two recent different methods have been used to improve the NLO χPT result [10, 11]. These promising methods can use as input the experimental Dalitz plot density information for the charged $\eta \to \pi^+\pi^-\pi^0$ channel. Their predictions provide a precise determination of Q, and also provide an important consistency check, namely to get a reasonable agreement with the experimental results for the neutral channel $\eta \to 3\pi^0$. As one of the main sources of uncertainty on Q comes from the uncertainty on the input parameters, it is crucial to precisely measure the density distribution of the $\eta \to \pi^+\pi^-\pi^0$ Dalitz plot.

1.1. Dalitz plot for the charged decay

Only few experiments since the 70s have measured the $\eta \to \pi^+\pi^-\pi^0$ Dalitz plot distribution. The results for the extracted Dalitz plot parameters are shown in Table I. This Dalitz plot is usually presented using the X and Y variables:

$$X = \sqrt{3}\,\frac{T_{\pi^+} - T_{\pi^-}}{Q_\eta} = \frac{\sqrt{3}}{2m_\eta Q_\eta}(u - t)\,,$$

$$Y = \frac{3T_{\pi^0}}{Q_\eta} - 1 = \frac{3}{2m_\eta Q_\eta}\left[(m_\eta - m_{\pi^0})^2 - s\right] - 1\,,$$

$$Q_\eta = T_{\pi^+} + T_{\pi^-} + T_{\pi^0} = m_\eta - 2m_{\pi^+} - m_{\pi^0}\,,$$

where T is the kinetic energy of the different pions in the η rest frame and s, t, u are the usual Mandelstam variables. The Dalitz plot parameters $a, b, c, \dots$, presented in the table, are defined by a polynomial expansion of the amplitude squared in X and Y, $|A(X,Y)|^2 \simeq N(1 + aY + bY^2 + cX + dX^2 + eXY + fY^3 + gX^2Y + hXY^2 + lX^3)$ [1].

As can be seen in Table I, there is some tension between the two most recent, high statistics experiments (KLOE [12] and WASA [13]), and more data is needed to provide a clearer picture. A new KLOE analysis, using an independent data set, a better understanding of the detector and improved analysis methods aims to provide a new measurement with reduced systematic uncertainties. The status and methodology of this analysis is presented here.

TABLE I

Experimental results for Dalitz plot parameters of $\eta \to \pi^+\pi^-\pi^0$.

Experiment	$-a$	b	d	f
Gormley(70) [14]	1.17(2)	0.21(3)	0.06(4)	—
Layter(73) [15]	1.080(14)	0.03(3)	0.05(3)	—
CBarrel(98) [16]	1.22(7)	0.22(11)	0.06(fixed)	—
KLOE(08) [12]	1.090(5)($^{+19}_{-8}$)	0.124(6)(10)	0.057(6)($^{+7}_{-16}$)	0.14(1)(2)
WASA(14) [13]	1.144(18)	0.219(19)(47)	0.086(18)(15)	0.115(37)

2. Signal event selection

The analysis is performed using 1.6 fb^{-1} of data collected with the KLOE detector in 2004–2005 (the previous analysis was based on 450 pb^{-1}). The KLOE detector is located in the DAΦNE ϕ-factory, and the η meson is

---

[1] The parameters c, e, h and l would signal a violation of charge conjugation invariance and are, therefore, usually fixed to zero in the fit of the Dalitz plot distribution.

produced via the radiative decay $\phi \to \eta\gamma_\phi$. For the $\eta \to \pi^+\pi^-\pi^0$ Dalitz plot analysis, with $\pi^0 \to \gamma\gamma$, we thus have two charged tracks and three photons in the final state. The event selection requires three clusters in the calorimeter [17] consistent with photons[2] and two tracks with opposite curvature in the drift chamber [18].

To improve the signal-to-background ratio several cuts are applied: on the angle between the tracks and the photons; on the time-of-flight used for particle identification; on the angle between the π^0 decay photons in the π^0 rest frame (Θ_{π^0}); and on the missing mass $\mathrm{MM}(\phi - \pi^+ - \pi^- - \gamma_\phi)$. The two last cuts are depicted in Fig. 2, where both data and Monte Carlo simulation are shown. These histograms are used to fix the scaling factors
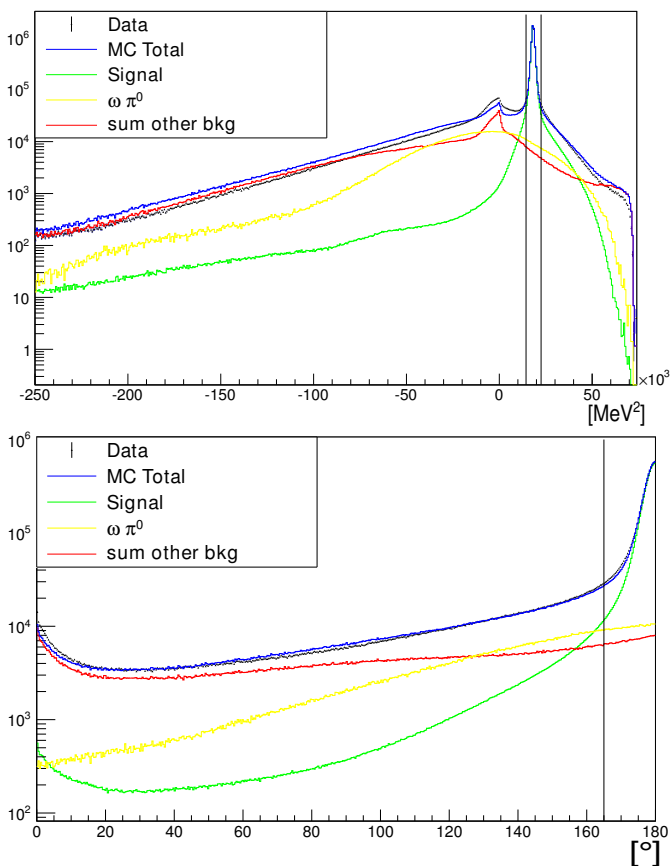

Fig. 2. Data–Monte Carlo comparison for the missing mass squared (top) and opening angle between π^0 photons in the π^0 rest frame (bottom). The vertical lines show the selection cuts.

---

[2] Not connected to a track and within the expected time window for a massless particle.

used for the Monte Carlo background, and, as can be seen in Fig. 2, a good data–Monte Carlo agreement is obtained. After reconstruction and cleanig cuts, the signal efficiency is 37.6% with a 1% background contamination, evaluated from Monte Carlo.

3. Fit of the Dalitz plot

The Dalitz plot parameters are obtained by a fit of the parametrization shown in Sec. 1.1 to the measured Dalitz plot density, by minimizing

$$\chi^2 = \sum_{i=1}^{N\,\text{bins}} \left(\frac{N_i - \sum_{j=1}^{N\,\text{bins}} \epsilon_j S_{ij} N_{\text{theory},j}}{\sigma_i} \right)^2 ,$$

where N_i is the background subtracted data content in Dalitz plot bin i, ϵ_j is the acceptance of bin j, S_{ij} is the smearing matrix from bin j to bin i, $N_{\text{theory},j} = \int |A(X,Y)|^2 dXdY$ (inside the phase space) is calculated with Monte Carlo integration for each bin, and σ_i, the error in bin i, includes the error in N_i and in $\epsilon_j S_{ij}$. Figure 3 shows the experimental Dalitz plot used.
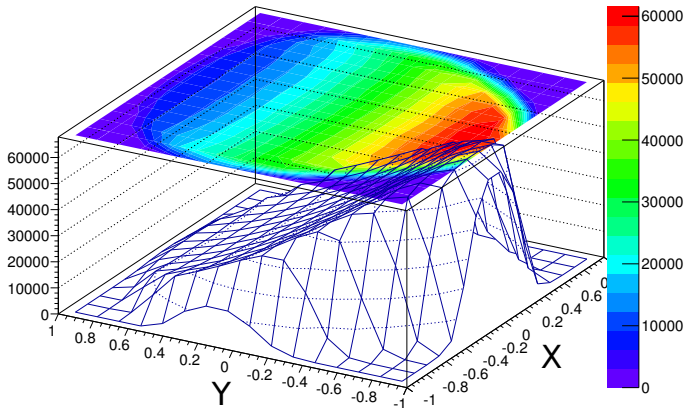

Fig. 3. Experimental Dalitz plot of $\eta \to \pi^+\pi^-\pi^0$.

From a detailed study both on data and Monte Carlo, fixing to zero the c and e parameters (and keeping the amplitude squared expansion up to the f term), it is found that the statistical uncertainty on the a, b, d and f parameters can be reduced by about a factor of two with respect to the previous KLOE result (see Table I), while improving also the systematic uncertainties.

The inclusion in the fit of the g parameter would also be possible and its impact on the stability of the result is currently under study.

In the near future, a further significant improvement of both statistical and systematic uncertainties of the Dalitz plot parameters will be possible at KLOE-2 [19], thanks to the luminosity upgrade of DAΦNE and to the better quality of reconstructed data using the new detectors: inner tracker [20], crystal calorimeters (CCALT) [21], and a tile calorimeter (QCALT) [22] of the upgraded KLOE detector.

REFERENCES

[1] D. Sutherland, *Phys. Lett.* **23**, 384 (1966).

[2] J. Bell, D. Sutherland, *Nucl. Phys.* **B4**, 315 (1968).

[3] R. Baur, J. Kambor, D. Wyler, *Nucl. Phys.* **B460**, 127 (1996).

[4] C. Ditsche, B. Kubis, U.-G. Meißner, *Eur. Phys. J.* **C60**, 83 (2009).

[5] H. Leutwyler, *Phys. Lett.* **B378**, 313 (1996).

[6] R. Dashen, *Phys. Rev.* **183**, 1245 (1969).

[7] J. Gasser, H. Leutwyler, *Nucl. Phys.* **B250**, 539 (1985).

[8] J. Beringer *et al.* [Particle Data Group], *Phys. Rev.* **D86**, 010001 (2012).

[9] J. Bijnens, K. Ghorbani, *J. High Energy Phys.* **0711**, 030 (2007).

[10] K. Kampf, M. Knecht, J. Novotný, M. Zdráhal, *Phys. Rev.* **D84**, 114015 (2011).

[11] G. Colangelo, S. Lanz, H. Leutwyler, E. Passemar, *PoS* **EPS-HEP2011**, 304 (2011).

[12] F. Ambrosino *et al.* [KLOE Collaboration], *J. High Energy Phys.* **0805**, 006 (2008).

[13] P. Adlarson *et al.* [WASA-at-COSY Collaboration], *Phys. Rev.* **C90**, 045207 (2014).

[14] M. Gormley *et al.*, *Phys. Rev.* **D2**, 501 (1970).

[15] J. Layter *et al.*, *Phys. Rev.* **D7**, 2565 (1973).

[16] A. Abele *et al.* [Crystal Barrel Collaboration], *Phys. Lett.* **B417**, 197 (1998).

[17] M. Adinolfi *et al.*, *Nucl. Instrum. Methods* **A482**, 364 (2002).

[18] M. Adinolfi *et al.*, *Nucl. Instrum. Methods* **A488**, 51 (2002).

[19] G. Amelino-Camelia *et al.*, *Eur. Phys. J.* **C68**, 619 (2010).

[20] A. Balla *et al.*, *JINST* **9**, C01014 (2014).

[21] F. Happacher, M. Martini, S. Miscetti, I. Sarra, *Nucl. Phys. B Proc. Suppl.* **197**, 215 (2009).

[22] M. Cordelli *et al.*, *Nucl. Instrum. Methods* **A617**, 105 (2010).